Hindawi
BioMed Research International
Volume 2019, Article ID 9835745, 14 pages
https://doi.org/10.1155/2019/9835745

Research Article

New Platinum(IV) and Palladium(II) Transition Metal Complexes of s-Triazine Derivative: Synthesis, Spectral, and Anticancer Agents Studies

Fatima A. I. Al-Khodir, Hana M. A. Abumelha, Tarfah Al-Warhi, and S. A. Al-Issa

Department of Chemistry, College of Science, Princess Nourah Bint Abdulrahman University, Saudi Arabia

Correspondence should be addressed to Fatima A. I. Al-Khodir; fatimaalkhodir@yahoo.com

Received 25 October 2018; Revised 1 January 2019; Accepted 31 January 2019; Published 17 February 2019

Academic Editor: Jinsong Ren

New Pd(II) and Pt(IV) triazine complexes $[Pt_3(\mathbf{L^1})_2(Cl)_9(H_2O)_3].3Cl.3H_2O$ (**1**), $[Pt_3(\mathbf{L^2})_2(Cl)_9(H_2O)_3].3Cl$ (**2**), $[Pt_3(\mathbf{L^3})_2(Cl)_9(H_2O)_3].3Cl$ (**3**), $[Pt_2(\mathbf{L^4})_2(Cl)_6(H_2O)_2]$ $.2Cl.4H_2O$ (**4**), $[Pd_3(\mathbf{L^1})_2(H_2O)_6]$ $.3Cl_2$ (**5**), $[Pd_3(\mathbf{L^2})_2(H_2O)_6].3Cl_2$ (**6**), $[Pd_3(\mathbf{L^3})_2(H_2O)_6].3Cl_2$ (**7**), and $[Pd_2(\mathbf{L^4})_2(H_2O)_4].2Cl_2$ (**8**) were synthesized and well characterized using elemental analyses, molar conductance, IR, UV-Vis, magnetic susceptibility, ^1H, ^{13}C-NMR spectra, and thermal analyses. These analyses deduced that the $\mathbf{L^1}$, $\mathbf{L^2}$, and $\mathbf{L^3}$ ligands act as tridentate forming octahedral geometry with Pt(IV) metal ions and square planar geometry in case of Pd(II) complexes but the $\mathbf{L^4}$ ligand acts as bidentate chelate. The molar conductance values refer to the fact that all the prepared s-triazine complexes have electrolyte properties which are investigated in DMSO solvent. Surface morphology behaviors of prepared complexes have been scanned using TEM. The crystalline behavior of triazine complexes has been checked based on X-ray powder diffraction patterns. The antimicrobial activity of the free ligands and their platinum(IV) and palladium(II) complexes against the species *Staphylococcus aureus* (G+), *Escherichia coli* (G−), *Aspergillus flavus*, and *Candida albicans* has been carried out and compared with the standard one. The coordination of ligands towards metal ions makes them stronger bacteriostatic agents, thus inhibiting the growth of bacteria and fungi more than the free ligands. The cytotoxic assessment IC_{50} of the free ligands and its platinum(IV) complexes *in vitro* against human colon and lung cancer cell lines introduced a promising efficiency.

1. Introduction

The s-triazine and its derivatives have a wide range of pharmaceutical benefits: antiviral, antimalarial, antibacterial, anti-inflammatory, antileukemia, anticancer, and anti-HIV activities [1–4]. Many triazine analogues are utilized as a building block for the construction of multisite ligand systems [5, 6]. A number of triazine analogues were tested for ion extraction of metal ions which have been reviewed [7, 8]. Some triazine derivatives with pyrazole, functioning at the least conventional habiliments, are screened and identified as potential inhibitors of photosynthetic electron transport [9]. In literature survey, it was refereed that the organic s-triazine's derivative compounds and transition metal complexes have been found to be effective in the field of nonlinear optical activity (NLO) [10–12] that can act as an auxiliary acceptor in NLO chromophores. Further advantages in considering the s-triazine as central moiety are its symmetric nature by which it will be possible to chemically tune its NLO nature by mono- or disubstitution [13, 14]. 1,3,5-Triazine is considered to be a remarkable in supramolecular chemistry since it can take part in all types of interactions, namely, coordination, hydrogen bonds, electrostatic and charge-transfer attractions, and aromatic-stacking interactions [15].

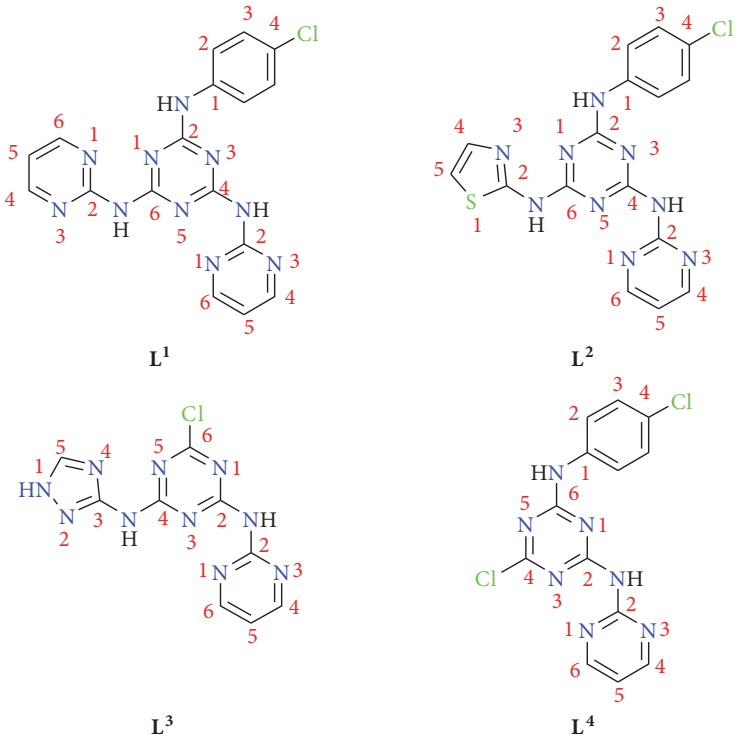

Figure 1: Structures of prepared triazine ligands [29]. ***L*^{1}**= *N*^{2}-(4-chlorophenyl)-*N*^{4},*N*^{6}-di(pyrimidin-2-yl)-1,3,5-triazine-2,4,6-triamine. ***L*^{2}**= *N*^{2}-(4-chlorophenyl)-*N*^{4},*N*^{6}-di(pyrimidin-2-yl)-1,3,5-triazine-2,4,6-triamine. ***L*^{3}**=6-chloro-*N*^{2}-(pyrimidin-2-yl)-*N*^{4}-(1H-1,2,4-triazol-3-yl)-1,3,5-triazine-2,4-diamine. ***L*^{4}**= 6-chloro-*N*^{2}-(4-chlorophenyl)-*N*^{4}-(pyrimidin-2-yl)-1,3,5-triazine-2,4-diamine).

Triazine derivatives have been widely used in several fields such as herbicide [16, 17]. In materials chemistry 1,3,5-triazine derivatives have been used as acceptors in star-shaped systems [18], liquid crystals [19], redox active chromophores [20], photovoltaic devices [21], and blue phosphorescent [22]. Also, it was used as functional materials [23], catalysts [24], absorption of surfactants [25], nanoporous membranes for desalination [26], and cathodes for lithium batteries [27, 28].

In connection of our previously work [29], this article aimed to synthesized new platinum(IV) and palladium(II) complexes with four triazine ligands (Figure 1) and checked the biological property and anticancer significance.

2. Materials and Methods

2.1. Chemicals. The $PtCl_4$ and $PdCl_2$ salts were received from Sigma-Aldrich Chemical Corporation, St. Louis, Mo, USA.

2.2. Synthesis of Trisubstituted s-Triazine Derivative Ligands. Synthesis of *N*^{2},*N*^{4},*N*^{6}-triaryl-1,3,5-triazine-2,4,6-triamine primary nucleus (Figure 2) was carried out as described in literature [30, 31]. The synthesis of **L**^{1}, **L**^{2}, **L**^{3}, and **L**^{4} triazine ligands was carried out according to our previously work [29], **L**^{1} prepared by stirring the mixtures of 2-aminopyrimidine with 6-chloro-N^2-(4-chlorophenyl)-N^4-di(pyrimidin-2-yl)-1,3,5-triazine-2,4-diamine in dioxane at refluxed temperature; **L**^{2} prepared by stirring the mixtures of 2-aminothiazole with 6-chloro-N^2-(4-chlorophenyl)-N^4-(pyrimidin-2-yl)-1,3,5-triazine-2,4-diamine in dioxane at refluxed temperature; **L**^{3} prepared by stirring the mixtures of 2-aminopyrimidine with 4,6-dichloro-N^2-(1H-1,2,4-triazol-3-yl)-1,3,5-triazin-2-amine in dioxane 50°C; **L**^{4} prepared by stirring the mixtures of 2-aminopyrimidine with 4,6-dichloro-N-(4-chlorophenyl)-1,3,5-triazin-2-amine in dioxane 50°C.

2.3. Synthesis of Pt(IV) and Pd(II) Complexes. A hot methanolic solution of the metal chloride (Pt(IV) and Pd(II)) (1 mM) was added to the hot methanolic solution of ligands (**L**^{1}, **L**^{2}, **L**^{3}, or **L**^{4}) (1 mM). The mixed solutions were stirred and refluxed at 70°C for 6 hrs. The colored precipitates thus separated out were washed with methanol and dried in *vacuo*.

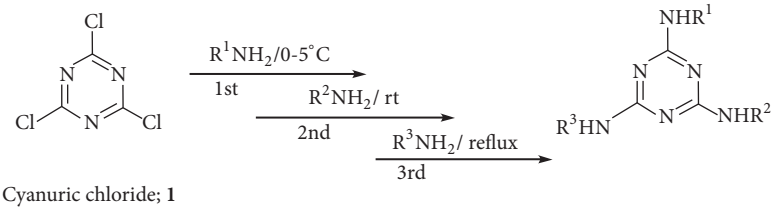

Cyanuric chloride; **1**

Figure 2: Synthesis of trisubstituted triazine derivatives.

2.4. Instrumentals

No.	Type of analysis	Model of the instruments
(i)	Elemental analyses	Perkin Elmer CHN 2400 (USA)
(ii)	Metal ions	gravimetrically
(iii)	Melting point	MPS10–120
(iv)	Molar conductivities	Jenway 4010 conductivity meter
(v)	Infrared spectra	Bruker Alpha FTIR Spectrophotometer
(vi)	UV-Vis absorption spectra	UV2 Unicam UV/Vis Spectrophotometer
(vii)	Magnetic moments	Magnetic Susceptibility Balance, Sherwood Scientific, Cambridge Science Park, Cambridge, England
(viii)	^{1}H,^{13}C-NMR spectra	Oxford YH-300 NMR spectrometer
(ix)	Mass spectra	70 eV using AEI MS 30 mass spectrometer
(x)	Thermal studies TG/DTG	Mettler Toledo AG thermogravimetric analyzer
(xi)	SEM	Quanta FEG 250 equipment
(xii)	XRD	X 'Pert PRO PANanalytical X-ray powder diffraction
(xiii)	TEM	JEOL 100s microscopy

2.5. Antimicrobial Study. Antimicrobial evaluations of the investigated samples were assessed by a modified Kirby-Bauer disc diffusion method [32, 33].

2.6. Anticancer Study. All tested samples were checked against human colon and lung cancer cell line by using neutral red (NR) technique [34].

3. Results and Discussion

3.1. Microanalytical and Physical Data. All the platinum(IV) and palladium(II) s-triazine derivative complexes were obtained as colored solids by the reaction of ligands (**L**^{1}, **L**^{2}, **L**^{3}, and **L**^{4}) with anhydrous metal chloride salts ($PtCl_4$ and $PdCl_2$). The experimental of elemental analyses of the ligands and their metal complexes (Table 1) are in good agreement with the calculated data. The ligands and their metal (IV/II) complexes are stable at room temperature and soluble in common organic solvents such as (DMSO and DMF). According to the elemental analysis and spectroscopic assignments, the chelating sites and geometry have been suggested and are displayed in Figure 3. The molar conductance of both free s-triazine derivative ligands and their Pt(IV) and Pd(II) complexes in 10^{-3} M of DMSO solution is in the range of 64.7–139.3 μS, which reveals the electrolytic behavior of the complexes [35]. Melting points of all complexes have values more than >300°C due to thermal stability properties.

3.2. FT-IR Spectra. Peaks at 1620, 1560, 1485, 740, and 627 cm^{-1} present in **L**^{1}, **L**^{2}, **L**^{3}, and **L**^{4} s-triazine derivatives ligands can be assigned for the $C{=}N_{pyrimidine}$, C=C, C=N, C–S, and C–Cl stretching vibrations. The FT-IR spectra of the ligands show a strong-to-medium strong bands at 1488 cm^{-1} (**L**^{1}), 1485 cm^{-1} (**L**^{2}), 1510 cm^{-1} (**L**^{3}), and 1484 cm^{-1} (**L**^{4}) which are assigned to ν(C=N) group of triazine [36]. Infrared spectral data of the **1**–**8** complexes (Table 2; Figure 4) usually a lot of valuable information is provided about the coordination mechanism. The free ligands which exhibit a band at 1623 cm^{-1} (**L**^{1}), 1619 cm^{-1} (**L**^{2}), 1621 cm^{-1} (**L**^{3}), and 1619 cm^{-1} (**L**^{4}) are assigned to ν(C=N) of pyrimidine and triazole rings. In case of complexes, this band is shifted to 1698–1667 cm^{-1} region attributed to nitrogen atom of (C=N) coordination to metal ion. The ligands shows a medium strong band at 1510–1484 cm^{-1}, which is characteristic of the ν(C=N) group in s-triazine [37, 38]. This band shifted to lower frequency of 1396–1382 cm^{-1} upon complexation which indicates that triazine ring nitrogen is one of the coordinating atoms in the ligand [38]. The ν(N–H) stretching frequency of pyrimidine/triazole rings exhibited at 3260–3112 cm^{-1} was shifted to lower wavenumbers after complexation due to the reduction of lone pair repulsive forces on the nitrogen atoms [39]. In the FT-IR spectra of complexes, the medium-weak bands appeared at 570–440 cm^{-1} regions

Table 1: Microanalytical and physicochemical data of ligands and their complexes.

Compounds*	Color	Λ(μS)	Elemental analyses found(Calc.)				Yield, %
			%C	%H	%N	%M	
1	Yellow	126.8	(21.44)	(2.01)	(14.71)	(30.73)	77
			21.32	1.96	14.57	30.66	
2	Brown	70.6	(20.66)	(1.63)	(13.55)	(31.46)	72
			20.54	1.54	13.50	31.32	
3	Green	64.7	(13.13)	(1.22)	(17.02)	(35.55)	71
			13.09	1.18	17.00	35.50	
4	Pale yellow	95.6	(22.64)	(2.19)	(14.22)	(28.29)	69
			22.56	2.13	14.16	28.11	
5	Dark brown	139.3	(28.64)	(2.69)	(19.65)	(22.39)	75
			28.56	2.57	19.54	22.31	
6	Red brown	82	(26.77)	(2.53)	(17.56)	(22.24)	70
			26.71	2.51	17.49	22.19	
7	Brownish green	106.7	(17.70)	(2.15)	(22.94)	(26.14)	74
			17.65	2.09	22.90	26.11	
8	Brown	122.3	(30.49)	(2.56)	(19.15)	(20.78)	71
			30.41	2.49	19.12	20.69	

* $[Pt_3(\mathbf{L^1})_2(Cl)_9(H_2O)_3].3Cl.3H_2O$ (**1**), $[Pt_3(\mathbf{L^2})_2(Cl)_9(H_2O)_3].3Cl$ (**2**), $[Pt_3(\mathbf{L^3})_2(Cl)_9(H_2O)_3].3Cl$ (**3**), $[Pt_2(\mathbf{L^4})_2(Cl)_6(H_2O)_2]$ $.2Cl.4H_2O$ (**4**), $[Pd_3(\mathbf{L^1})_2(H_2O)_6].3Cl_2$ (**5**), $[Pd_3(\mathbf{L^2})_2(H_2O)_6].3Cl_2$ (**6**), $[Pd_3(\mathbf{L^3})_2(H_2O)_6]$ $.3Cl_2$ (**7**) and $[Pd_2(\mathbf{L^4})_2(H_2O)_4].2Cl_2$ (**8**).

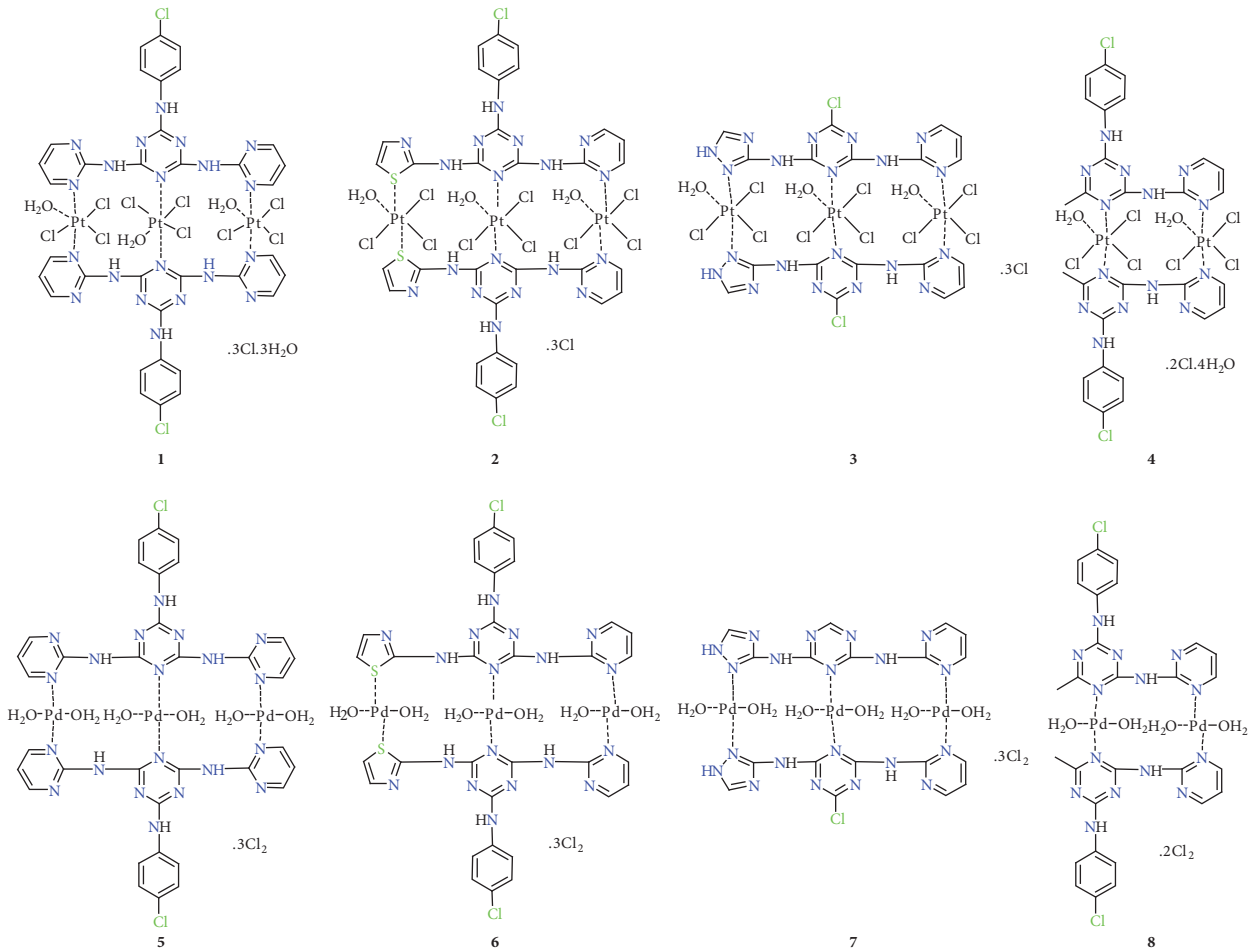

Figure 3: Suggested structures of Pt(IV) and Pd(II) complexes.

Table 2: FT-IR spectral band assignments of $\mathbf{L^1}$, $\mathbf{L^2}$, $\mathbf{L^3}$, and $\mathbf{L^4}$ ligands and their complexes.

Compounds	FTIR spectral assignments (cm^{-1})				
	ν(N–H)	$\nu(C=N)_{aromatic}$	$\nu(C=C)_{aromatic}$	$\nu(C=N)_{triazine}$	ν(M–N)
$\mathbf{L^1}$	3249-3112	1623	1559	1488	-
$\mathbf{L^2}$	3260-3142	1619	1555	1485	-
$\mathbf{L^3}$	3251-3156	1621	1586	1510	-
$\mathbf{L^4}$	3244-3150	1619	1574	1484	-
1	3200	1679	1560	1385	545, 447
2	-	1667	1537	1383	536, 441
3	-	1698	1585	1382	570, 470
4	-	1695	1567	1390	530, 469
5	-	1689	1530	1394	537, 440
6	-	1695	1557	1396	540, 463
7	-	1698	1550	1391	537, 467
8	-	1691	1537	1393	537, 463

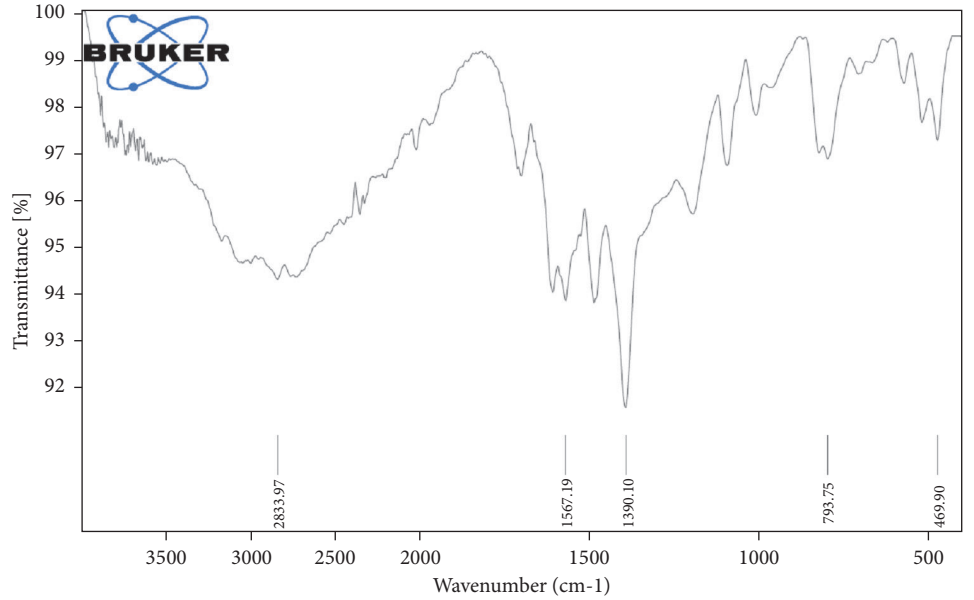

(a)

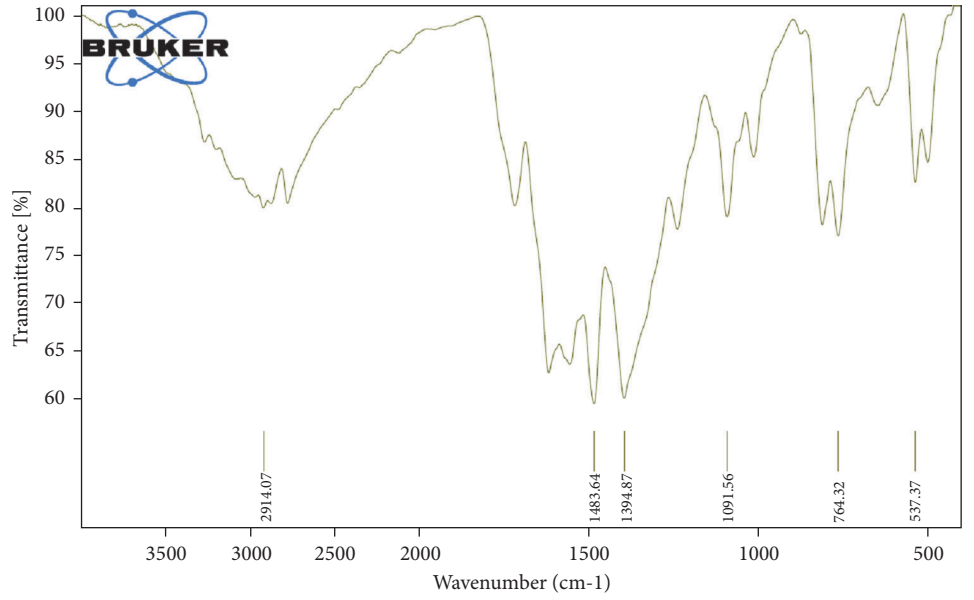

(b)

Figure 4: FT-IR spectra of (a) $[Pt_2(\mathbf{L^4})_2(Cl)_6(H_2O)_2].2Cl.4H_2O$ (**4**) and (b) $[Pd_3(\mathbf{L^2})_2\ (H_2O)_6].3Cl_2$ (**6**).

which can be assigned to ν(M–N) [40] and confirm the interaction between metal and ligand.

3.3. Electronic and Magnetic Studies. The electronic spectra of $[Pt_3(\mathbf{L^1})_2(Cl)_9(H_2O)_3].3Cl.3H_2O$ (**1**), $[Pt_3(\mathbf{L^2})_2(Cl)_9(H_2O)_3].3Cl$ (**2**), $[Pt_3(\mathbf{L^3})_2(Cl)_9(H_2O)_3].3Cl$ (**3**), and $[Pt_2(\mathbf{L^4})_2(Cl)_6(H_2O)_2]$.$2Cl.4H_2O$ (**4**) complexes which displayed charge-transfer transitions may interfere and prevent the observation of all the expected bands [41, 42].The distinct bands at 300–311 and 337–396 cm^{-1} are attributed to a combination of metal ligand charge transfer (M$\longrightarrow$ L_{CT}) and d–d transition band. The other weak band at 429–437 cm^{-1} is attributed to combination of N$\longrightarrow$Pt(IV) metal charge transfer ($L\pi \longrightarrow M_{CT}$) and d–d transition bands. The Pt(IV) complexes are found to be diamagnetic character, so the Pt(IV) complexes must be octahedral geometry. The Pt(IV) is d^6 system and four bands are expected due to $^1A_{1g} \longrightarrow {}^3T_{1g}$, $^1A_{1g} \longrightarrow {}^3T_{2g}$, $^1A_{1g} \longrightarrow {}^1T_{1g}$, and $^1A_{1g} \longrightarrow {}^1T_{2g}$ transitions. The shift to lower frequency after complexation is due to the binding between Pt(IV) ion nitrogen atom of triazine, pyrimidine, thiazole, and triazole rings. Palladium(II) complexes have diamagnetic properties. The electronic absorption spectra of palladium(II) complexes have distinguished bands at (300 nm), (312 and 352 nm), (309, 334 and 391 nm), and (296, and 339 nm) for $\mathbf{L^1}$, $\mathbf{L^2}$, $\mathbf{L^3}$, and $\mathbf{L^4}$ ligands, respectively, due to Pd-$L^n{}_{CT}$ charge-transfer transitions.

3.4. ^1H, ^{13}C-NMR Spectra

*Complex **1***. ^{1}H-NMR (DMSO-d_6): δ = 7.26 (t, H, J = 4.5 Hz, pyrimidine C_5H), 7.30 (t, H, J = 4.5 Hz, pyrimidine C_5H), 7.34 (d, 2H, J = 4.5 Hz, p-Chloroaniline C_3H), 7.39 (d, 2H, J = 9.9 Hz, p-Chloroaniline C_2H), 8.81 (d, 2H, J = 4.5 Hz, pyrimidine $C_{4,6}H$), 8.91 (d, 2H, J = 4.5 Hz, pyrimidine $C_{4,6}H$), 9.82 (s, 1H, NH), 11.19 (s, 1H, NH), 12.06 (s, 1H, NH). ^{13}C-NMR (DMSO-d_6): δ = 111.4, 113.8, 117.9, 123.9, 130.7, 140.1, 144.1, 147.5, 153.1, 157.1, 159.2, 163.4, 163.9, 166.2, and 169.7 (Ar-C, C=C, C=N).

*Complex **2***. ^{1}H-NMR (DMSO-d_6): δ = 7.34 (d, 2H, J = 7.2 Hz, thiazole C_5H), 7.38 (t, 4H, J = 4.5 Hz, pyrimidine C_5H), 7.44 (d, 4H, J = 4.5 Hz, p-Chloroaniline C_3H), 7.77 (d, 4H, J = 9.9 Hz, p-Chloroaniline C_2H), 7.86 (d, 2H, J = 6.3 Hz, thiazole C_4H), 8.09 (d, 4H, J = 4.5 Hz, pyrimidine $C_{4,6}H$), 9.51 (s, 2H, NH), 11.18 (s, 2H, NH), 12.08 (s, 2H, NH). ^{13}C-NMR (DMSO-d_6): δ = 112.5, 114.0, 114.9, 123.2, 132.5, 145.2, 151.4, 152.9, 155.4, 157.0, 158.8, 162.0, 163.5, and 172.2 (Ar-C, C=C, C=N, C-S).

*Complex **3***. ^{1}H-NMR (DMSO-d_6): δ = 7.23 (t, 2H, J = 4.5 Hz, pyrimidine C_5H), 7.32 (s, 2H, triazole C_5H), 8.45 (d, 4H, J = 4.5 Hz, pyrimidine $C_{4,6}H$), 8.91 (s, 2H, NH), 11.22 (s, 2H, NH), 11.46 (s, 1H, NH). ^{13}C-NMR (DMSO-d_6): δ = 115.8, 142.8, 146.5, 155.0, 156.2, 159.2, 163.8, 163.9, and 167.1 (Ar-C, C=C, C=N, C-Cl).

*Complex **4***. ^{1}H-NMR (DMSO-d_6): δ = 7.35 (t, 4H, J = 4.5 Hz, pyrimidine C_5H), 7.39 (d, 4H, J = 4.5 Hz, p-Chloroaniline C_3H), 7.44 (d, 4H, J = 9.9 Hz, p-Chloroaniline C_2H), 7.76 (d, 4H, J = 4.5 Hz, pyrimidine $C_{4,6}H$), 9.50 (s, 2H, NH), 11.19 (s, 2H, NH). ^{13}C-NMR (DMSO-d_6): δ = 111.9, 118.0, 123.1, 132.4, 144.4, 147.9, 153.5, 156.8, 161.8, 166.6, and 172.1 (Ar-C, C=C, C=N, C-Cl).

*Complex **5***. ^{1}H-NMR (DMSO-d_6): δ = 7.32 (t, 2H, J = 4.5 Hz, pyrimidine C_5H), 7.35 (t, 2H, J = 4.5 z, pyrimidine C_5H), 7.41 (d, 4H, J = 4.5 Hz, p-Chloroaniline C_3H), 7.46 (d, 4H, J = 9.9 Hz, p-Chloroaniline C_2H), 8.57 (d, 4H, J = 4.5 Hz, pyrimidine $C_{4,6}H$), 7.79 (d, 4H, J = 4.5 Hz, pyrimidine $C_{4,6}H$), 9.55 (s, 2H, NH), 11.19 (s, 2H, NH), 11.20 (s, 2H, NH). ^{13}C-NMR (DMSO-d_6): δ = 113.1, 115.1, 120.1, 123.8, 129.4, 141.7, 147.0, 149.8, 152.4, 157.7, 159.6, 163.1, 163.9, 165.8, and 171.1 (Ar-C, C=C, C=N).

*Complex **6***. ^{1}H-NMR (DMSO-d_6): δ = 7.33 (d, 2H, J = 7.2 Hz, thiazole C_5H), 7.36 (t, 4H, J = 4.5 Hz, pyrimidine C_5H), 7.45 (d, 4H, J = 4.5 Hz, p-Chloroaniline C_3H), 7.78 (d, 4H, J = 9.9 Hz, p-Chloroaniline C_2H), 7.81 (d, 2H, J = 6.3 Hz, thiazole C_4H), 8.12 (d, 4H, J = 4.5 Hz, pyrimidine $C_{4,6}H$), 9.55 (s, 2H, NH), 11.20 (s, 2H, NH), 12.02 (s, 2H, NH). ^{13}C-NMR (DMSO-d_6): δ = 110.2, 113.1, 115.8, 123.8, 131.8, 146.1, 150.3, 152.1, 155.0, 156.6, 158.1, 161.2, 163.1, and 173.4 (Ar-C, C=C, C=N, C-S).

*Complex **7***. ^{1}H-NMR (DMSO-d_6): δ = 7.21 (t, 2H, J = 4.5 Hz, pyrimidine C_5H), 7.39 (s, 2H, triazole C_5H), 8.46 (d, 4H, J = 4.5 Hz, pyrimidine $C_{4,6}H$), 8.92 (s, 2H, NH), 11.20 (s, 2H, NH), 11.48 (s, 1H, NH). ^{13}C-NMR (DMSO-d_6): δ = 116.5, 141.9, 147.4, 154.4, 155.9, 159.8, 163.1, 164.5, and 168.8 (Ar-C, C=C, C=N, C-Cl).

*Complex **8***. ^{1}H-NMR (DMSO-d_6): δ = 7.33 (t, 4H, J = 4.5 Hz, pyrimidine C_5H), 7.36 (d, 4H, J = 4.5 Hz, p-Chloroaniline C_3H), 7.46 (d, 4H, J = 9.9 Hz, p-Chloroaniline C_2H), 7.81 (d, 4H, J = 4.5 Hz, pyrimidine $C_{4,6}H$), 9.55 (s, 2H, NH), 11.20 (s, 2H, NH). ^{13}C-NMR (DMSO-d_6): δ = 113.5, 119.2, 122.9, 130.5, 145.5, 149.4, 153.1, 157.4, 162.7, 165.6, and 171.8 (Ar-C, C=C, C=N, C-Cl).

The ^{1}H-NMR spectral data of the synthesized Pt(IV) and Pd(II) complexes have been shifted to downfield because of formation metal chelating through the nitrogen atoms of triazine, pyrimidine, thiazole, and triazole rings.

3.5. Thermogravimetric Studies. Thermal analyses (TG-DTG) were performed under N_2 atmosphere. The thermogravimetric and differential thermogravimetric curves of the synthesized Pt(IV) (**1**–**4**) and Pd(II) (**5**–**8**) complexes are shown in Figures 5 and 6. Table 3 refereed to the thermal decomposition assignments of all complexes from room temperature till 1000°C.

3.6. X-Ray Diffraction Spectra. XRD diffraction patterns of the solid Pt(IV) and Pd(III) triazine complexes have been displayed in Figure 7. The diffraction patterns of new Pt(IV) and Pd(II) complexes at 2θ values are (11.094, 13.585, 15.041, 15.840, 19.929, 22.276, 23.198, 30.360, 33.693, 39.780, 47.720°), (5.082, 12.894, 19.845, 29.786°), (12.861, 16.426, 17.438, 19.695, 22.031, 26.390, 35.265°), (13.078, 19.773, 29.893, 35.342, 45.307°), (16.712, 27.173, 28.562, 31756, 37.958, 45.472, 56.157, 57.440, 59.071°), (4.948, 10.051, 13.820, 16.705, 17.357, 19.608, 20.512, 24.738, 26.567, 27.247, 29.786, 37.806, 56.168,

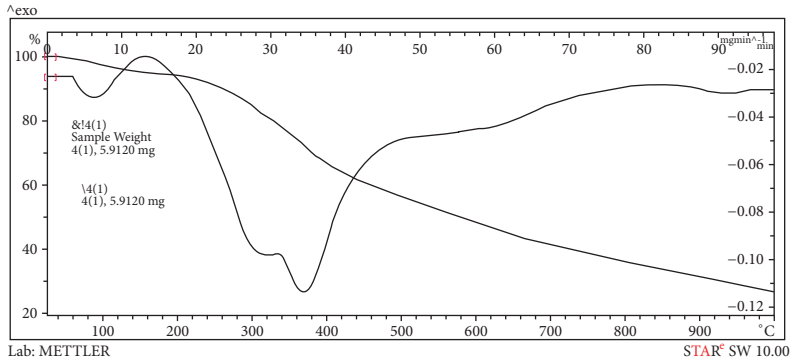

(a) Complex **1**

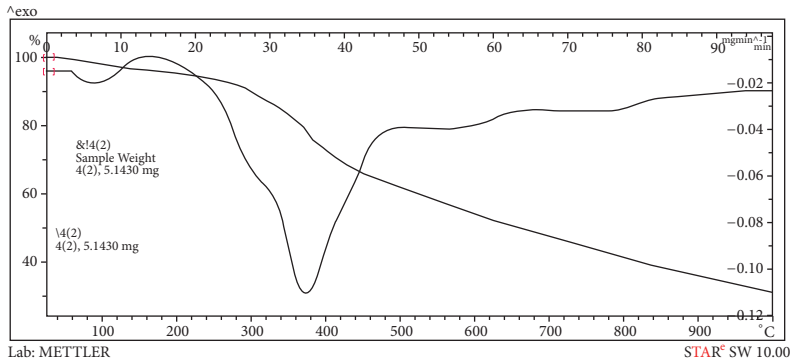

(b) Complex **2**

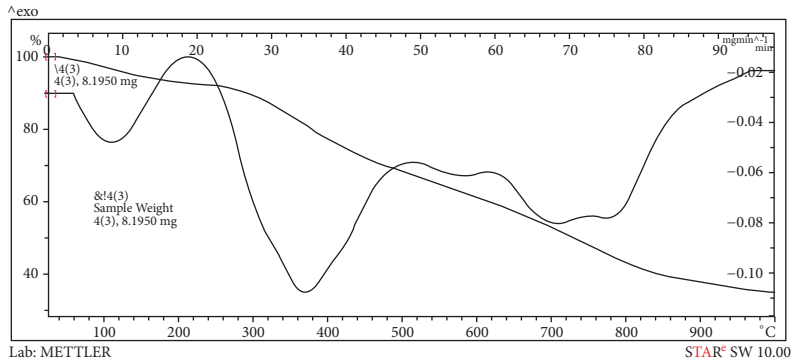

(c) Complex **3**

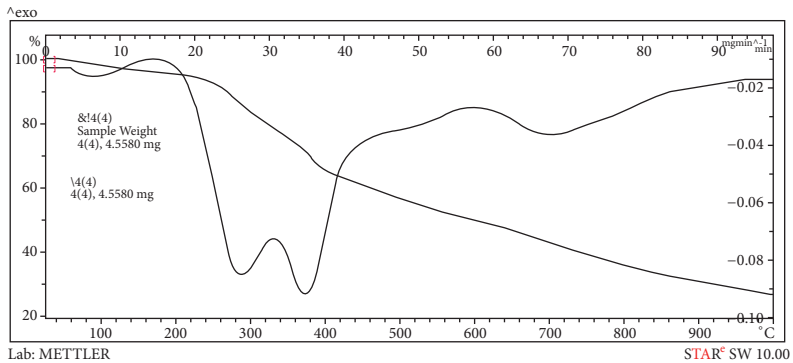

(d) Complex **4**

Figure 5: TGA-DTG curves of Pt(IV) complexes **1**–**4**.

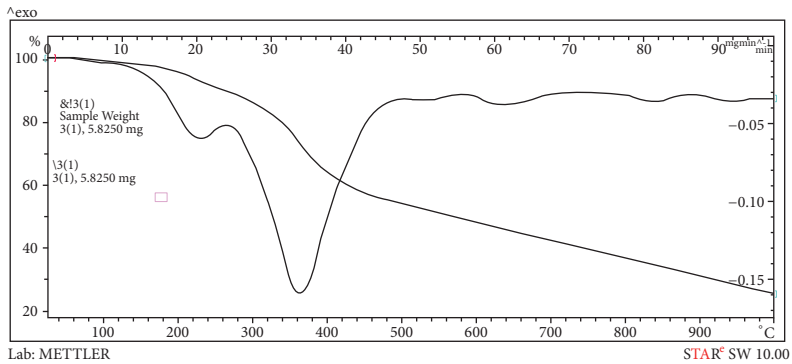

(a) Complex **5**

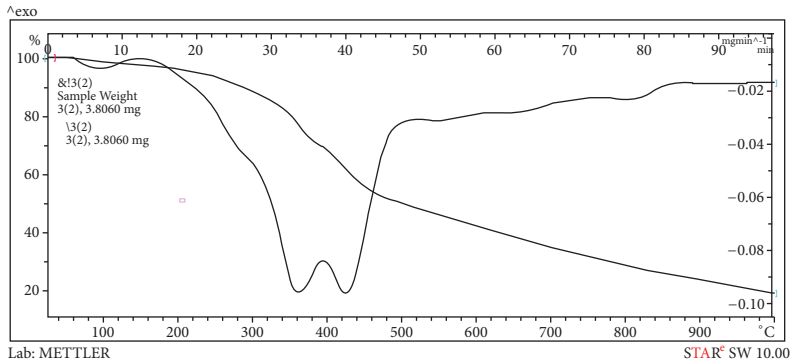

(b) Complex **6**

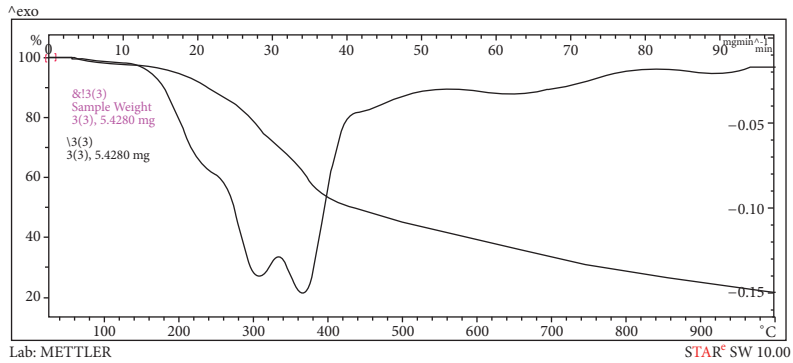

(c) Complex **7**

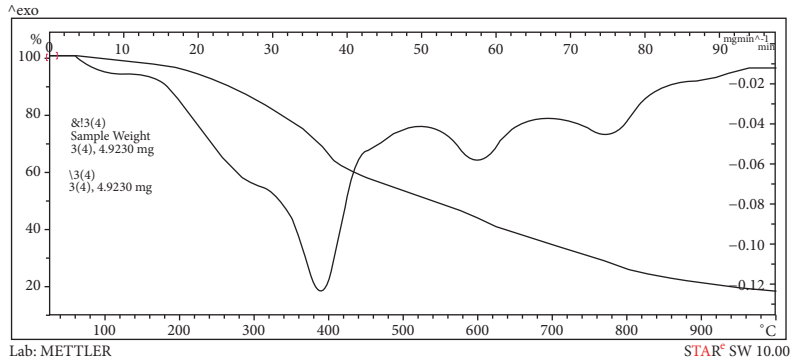

(d) Complex **8**

Figure 6: TGA-DTG curves of Pd(II) complexes **5**–**8**.

Table 3: Thermo gravimetric data of Pt(IV) and Pd(II) triazine complexes.

Complexes	DTG_{max}	Total weight loss		Total residual	
		Weight loss, %	Assignments	Residue, %	Assignments
1	100 300, 380, 600	74	$3H_2O$ uncoord $2\mathbf{L}^1+6Cl_2$	26	PtO_2 + Few carbons
2	100 310, 380, 580	70	$3H_2O$ coord $2\mathbf{L}^2+6Cl_2$	30	PtO_2 + Few carbons
3	100 370, 580, 700	68	$3H_2O$ coord $2\mathbf{L}^3+6Cl_2$	32	PtO_2 + Few carbons
4	100 280, 380, 700	72	$4H_2O$ uncoord $2\mathbf{L}^4+4Cl_2+2H_2O$	28	PtO_2 + Few carbons
5	230, 360, 620	75	$2\mathbf{L}^1+3Cl_2+6H_2O$	25	PdO + Few carbons
6	360, 420, 800	75	$2\mathbf{L}^2+3Cl_2+6H_2O$	25	PdO + Few carbons
7	300, 360, 650	78	$2\mathbf{L}^3+3Cl_2+6H_2O$	22	PdO + Few carbons
8	380, 620, 800	82	$2\mathbf{L}^4+2Cl_2+4H_2O$	18	PdO + Few carbons

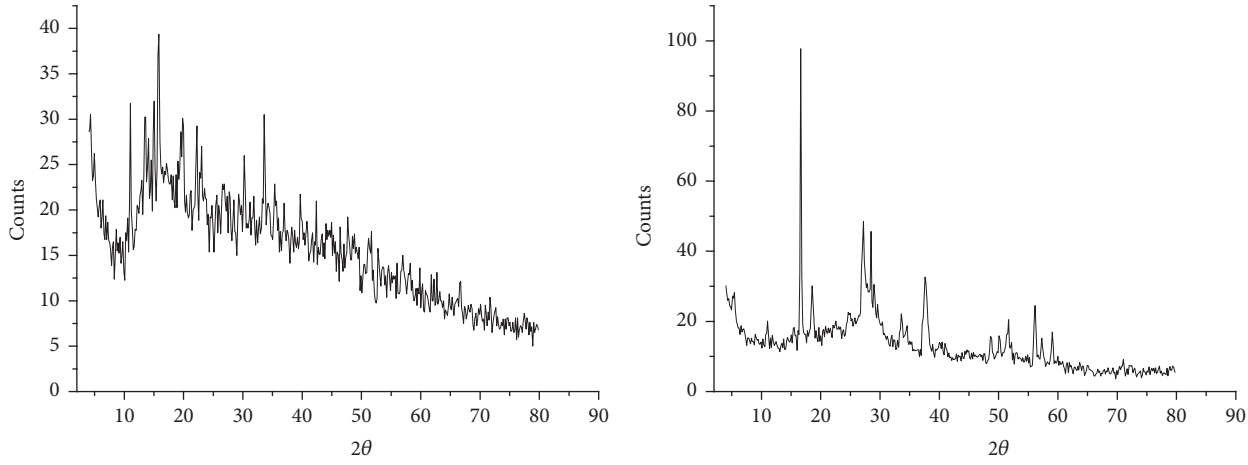

(a) XRD patterns of $[Pt_3(\mathbf{L}^1)_2(Cl)_9(H_2O)_3].3Cl.3H_2O$ (**1**) complex

(b) XRD patterns of $[Pd_3(\mathbf{L}^3)_2(H_2O)_6]\ .3Cl_2$ (**7**) complex

Figure 7

57.332, 59.199°), (5.527, 11.110, 16.704, 18.605, 27.263, 28.547, 29.090, 33.708, 37.678, 51.690, 56.690, 56.193, 57.367, 59.096, 79.472°), and (16.839, 27.384, 28.680, 37.851, 48.826, 50.279, 56.287, 57.573, 59.194°) for the complexes **1**–**8**, respectively. The particle size was estimated using Scherrer's equation [43]. The XRD patterns due to metallic platinum are agreement with JCPDS PDF card no. 04-0802 standard card [44] with (111), (200), (220) planes, respectively. Powder XRD patterns of Pd(II) complexes are shown in Figure 7. These spectra included distinguish patterns at 2θ = 37.678, 51.690, 59.096, and 79.472° assigned to (111), (200), (220), and (311) of Pd metal with fcc structure matching with JCPDS file no. 87-0638 [45]. This result confirms the presence of metallic Pd with fcc structure. The grain sizes of platinum(IV) and palladium(II) complexes are existed within 42–50 and nm according to highest distinguish peaks.

3.7. Scanning and Transmission Electron Microscopes. The SEM photos of Pt(IV) and Pd(II) complexes **1**–**8** are shown in Figure 8. These images reveal that the surface of all complexes is homogeneous with various morphological view because of the role of Pt(IV) and Pd(II) metal ions in the rearrangement of grains.

According to the TEM technique (Figure 9), the average of particle size of platinum(IV) complexes existed within 15–92 nm.

3.8. Biological Studies

3.8.1. Antibacterial Assessments. Table 4 refers to the antibacterial activity of the free triazine ligands ($\mathbf{L}^1$, $\mathbf{L}^2$, $\mathbf{L}^3$, and $\mathbf{L}^4$) comparable with its platinum(IV) and palladium(II) complexes (**1**–**8**) against *Staphylococcus aureus* (G+), *Escherichia coli* (G−), and fungi (*Aspergillus flavus* and *Candida albicans*). All complexes beside the four free ligands which have not any significant inhibitory against both respected fungi except for complexes of **1**, **3**, **5**, **7,** and **8** have moderate inhibitory against *Aspergillus flavus*. All complexes have a moderate bacterial inhibitory in comparison with ampicillin standard drug. The variation in the activity of different metal complexes against different microorganisms depends on either the impermeability of the cells of the microbes or the differences in ribosomes in microbial cells [46, 47].

3.8.2. Anticancer Assessments. Table 5 and Figure 10 refer to the IC_{50} results of the free triazine ligands and its Pt(IV) complexes. From these data, it is clearly deduced that the

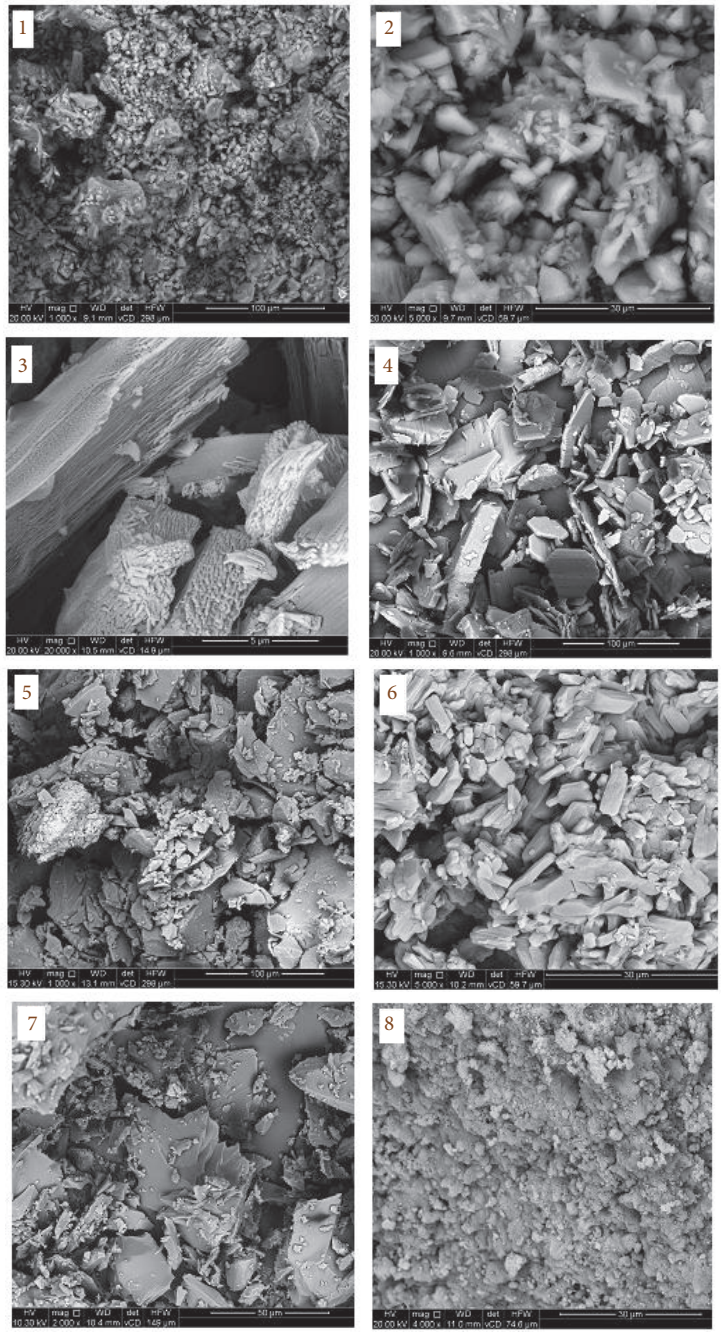

Figure 8: SEM photos of Pt(IV) and Pd(II) complexes **1**–**8**.

Table 4: Inhibition zone diameter of free ligands and its Pt(IV) and Pd(II) complexes.

Sample		Inhibition zone diameter (mm/mg Sample)			
		Bacteria		Fungi	
		Escherichia coli (G^-)	*Staphylococcus aureus* (G^+)	*Aspergillus flavus* (Fungus)	*Candida albicans* (Fungus)
Standard	Ampicillin: Antibacterial agent	30	24	--	--
	Amphotericin B: Antifungal agent	--	--	16	21
Control: DMSO		0.0	0.0	0.0	0.0
L[1]		11	10	10	0.0

Table 4: Continued.

Sample	Inhibition zone diameter (mm/mg Sample)			
	Bacteria		Fungi	
	Escherichia coli (G^-)	*Staphylococcus aureus* (G^+)	*Aspergillus flavus* (Fungus)	*Candida albicans* (Fungus)
L^2	0.0	0.0	0.0	0.0
L^3	0.0	0.0	0.0	0.0
L^4	15	10	0.0	0.0
1	19	18	16	0.0
2	12	11	0.0	0.0
3	24	23	12	0.0
4	14	12	0.0	0.0
5	14	15	15	0.0
6	11	11	0.0	0.0
7	16	17	12	0.0
8	14	15	11	0.0

∗Ampicillin and amphotericin B are standards of antibacterial and antifungal agents.

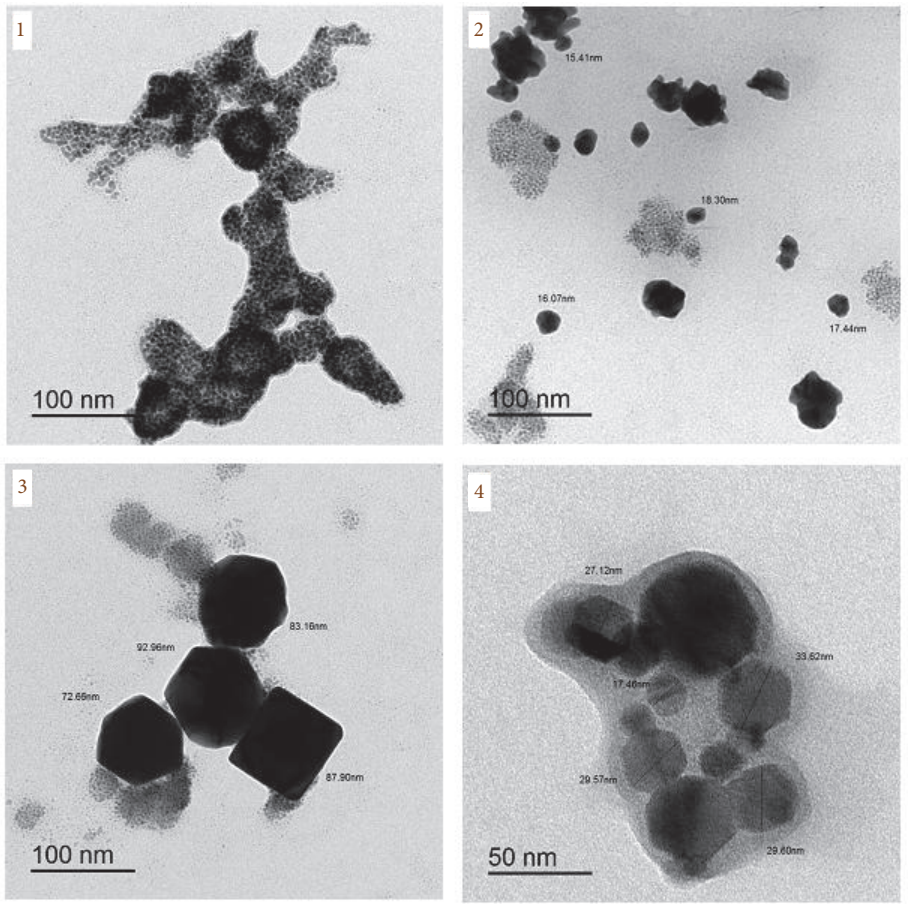

Figure 9: TEM photos of Pt(IV) complexes **1**–**4**.

Table 5: IC_{50} activity of the free ligands and its Pt(IV) complexes.

Against human colon cancer cell lines								
Concentration (μg/mL)	Viability (%)							
	$\mathbf{L^1}$	**1**	$\mathbf{L^2}$	**2**	$\mathbf{L^3}$	**3**	$\mathbf{L^4}$	**4**
100	65	66	61	72.7	55.3	6.4	35.5	44.6
50	70	67.8	64.4	81.7	60	31.8	41.4	56.6
10	72	70	69.3	82.5	65	62.9	66.8	71.5
IC_{50}	170	461	277	259	162.8	27	50.7	79
Against human lung cancer A549 cell lines								
Concentration (μg/mL)	Viability (%)							
	$\mathbf{L^1}$	**1**	$\mathbf{L^2}$	**2**	$\mathbf{L^3}$	**3**	$\mathbf{L^4}$	**4**
150	82.4	100	96	100	100	44.6	100	77.7
100	83.4	100	98.7	100	100	61.7	100	100
50	86	100	100	100	100	66.5	100	100
10	98.7	100	100	100	100	100	100	100
IC_{50}	431.4	-	1305.7	-	-	128	-	212

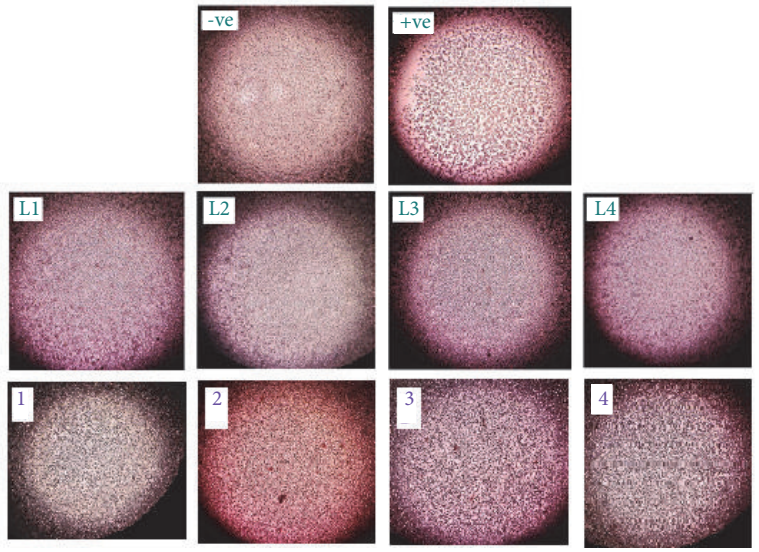

(a) Images of the neutral red cytotoxicity test of the free $\mathbf{L^1}$, $\mathbf{L^2}$, $\mathbf{L^3}$, and $\mathbf{L^4}$ ligands and their Pt(IV) complexes (**1–4**) against human colon cancer cell lines

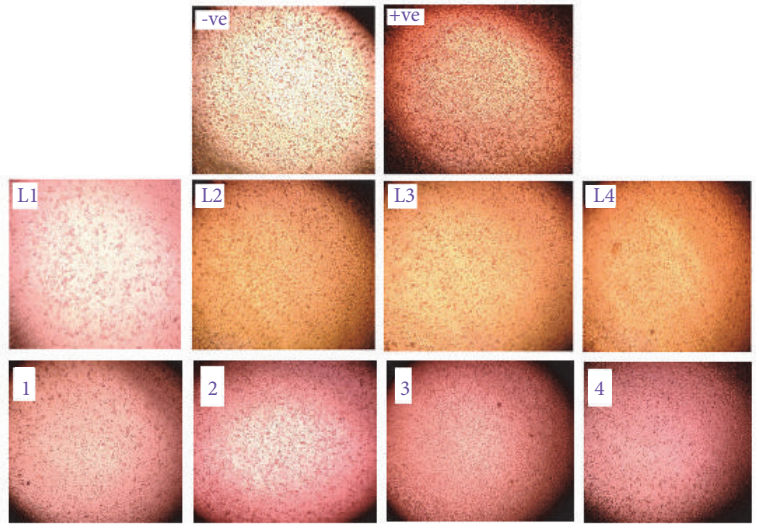

(b) Images of the neutral red cytotoxicity test of the free $\mathbf{L^1}$, $\mathbf{L^2}$, $\mathbf{L^3}$, and $\mathbf{L^4}$ ligands and their Pt(IV) complexes (**1–4**) against human lung cancer A549 cell lines

Figure 10

$[Pt_3(\mathbf{L}^3)_2(Cl)_9(H_2O)_3].3Cl$ (**3**) complex has an efficiency against human colon and human lung cancer A549 cell lines rather than its corresponding free $\mathbf{L}^3$ ligand.

Data Availability

The data used to support the findings of this study are available from the corresponding author upon request.

Conflicts of Interest

The authors declare that they have no conflicts of interest.

Acknowledgments

This work was funded by the Deanship of Scientific Research at Princess Nourah bint Abdulrahman University. The authors would like to thank Professor Dr. Ibrahim A. Alsarra for his scientific guidance; also they would like to thank the Assistant Researcher Mrs. Lina Almaliky for her participation in the preparation of experimental work in lab.

References

[1] N. Lolak, S. Akocak, S. Bua, and C. T. Supuran, "Design, synthesis and biological evaluation of novel ureido benzenesulfonamides incorporating 1, 3, 5-triazine moieties as potent carbonic anhydrase IX inhibitors," *Bioorganic Chemistry*, vol. 82, pp. 117–122, 2019.

[2] J. Verhoeven, B. N. Reddy, L. Meerpoel, J. W. Thuring, and G. Verniest, "Synthesis and transformations of pyrrolo[1,2-a][1,3,5]-triazines," *Tetrahedron Letters*, vol. 59, no. 52, pp. 4537–4539, 2018.

[3] G. Wang, Z. Peng, Z. Gong, and Y. Li, "Synthesis, biological evaluation, and docking studies of novel 5,6-diaryl-1,2,4-triazine thiazole derivatives as a new class of α-glucosidase inhibitors," *Bioorganic Chemistry*, vol. 78, pp. 195–200, 2018.

[4] M. Arshad, A. R. Bhat, K. K. Hoi, I. Choi, and F. Athar, "Synthesis, characterization and antibacterial screening of some novel 1,2,4-triazine derivatives," *Chinese Chemical Letters*, vol. 28, no. 7, pp. 1559–1565, 2017.

[5] J. Chu, W. Chen, G. Su, and Y. Song, "Four new copper(II) complexes with di-substituted s-triazine-based ligands," *Inorganica Chimica Acta*, vol. 376, no. 1, pp. 350–357, 2011.

[6] C. Diaz and I. Izquierdo, "Iron and ruthenium derivatives of cyclophosphazenes coordinated through nitrile spacer ligands," *Polyhedron*, vol. 18, no. 10, pp. 1479–1484, 1999.

[7] L. M. Harwood, M. J. Hudson, M. G. Drew, and F. W. Lewis, "Highly efficient separation of actinides from lanthanides by a phenanthroline-derived bis-triazine ligand," *Journal of the American Chemical Society*, vol. 133, pp. 13093–13102, 2011.

[8] D. X. Wang and M. X. Wang, "Anion–π Interactions: Generality, Binding Strength, and Structure," *Journal of the American Chemical Society*, vol. 135, no. 2, pp. 892–897, 2013.

[9] A. D. Tiwari, A. K. Mishra, S. B. Mishra, B. B. Mamba, B. Maji, and S. Bhattacharya, "Synthesis and DNA binding studies of Ni(II), Co(II), Cu(II) and Zn(II) metal complexes of N^1,N^5-bis[pyridine-2-methylene]-thiocarbohydrazone Schiff-base ligand," *Acta PartA*, vol. 79, pp. 1050–1056, 2011.

[10] T. C. Shehee, R. E. Sykora, P. S. Halasyamani, and T. E. Albrecht Schmitt, "Hydrothermal preparation, structures, and NLO properties of the rare earth molybdenyl iodates, RE (MoO2)(IO3) 4 (OH)[RE= Nd, Sm, Eu]," *Inorganic Chemistry*, vol. 42, pp. 457–463, 2003.

[11] H. Lee, D. Kim, H. K. Lee et al., "Discotic liquid crystalline materials for potential nonlinear optical applications: synthesis and liquid crystalline behavior of 1,3,5-triphenyl-2,4,6-triazine derivatives containing achiral and chiral alkyl chains at the periphery," *Tetrahedron Letters*, vol. 45, no. 5, pp. 1019–1022, 2004.

[12] R. Boese, G. R. Desiraju, R. K. Jetti et al., "Crystal structures and packing of 2,4,6-tris(4-fluorophenoxy)-1,3,5-triazine and 2,4,6-tris(3,4-dimethylphenoxy)-1,3,5-triazine. New materials for octupolar nonlinear optics," *Structural Chemistry*, vol. 13, pp. 321–328, 2002.

[13] L. Xiang, Y. G. Liu, A. G. Jiang, and D. Y. Huang, "Theoretical investigation of s-triazine derivatives as novel second-order nonlinear optical chromophores," *Chemical Physics Letters*, vol. 338, pp. 167–172, 2001.

[14] G. Park and B. R. Cho, "First hyperpolarizabilities of triazine derivatives. Ab initio studies and Hammett correlation," *Journal of Physical Organic Chemistry*, vol. 17, pp. 169–177, 2004.

[15] T. J. Mooibroek and P. Gamez, "The s-triazine ring, a remarkable unit to generate supramolecular interactions," *Inorganica Chimica Acta*, vol. 360, no. 1, pp. 381–404, 2007.

[16] Z. Zhang, N. Li, K. Wang et al., "Dispersant-assisted dynamic microwave extraction of triazine herbicides from rice," *Analytical Methods*, no. 18, pp. 3788–3794, 2018.

[17] H. Tian, C. Xu, J. Cai, and J. Xu, "The aqueous biphasic system based on cholinium ionic liquids and nonionic surfactant and its application for triazine-based herbicides extraction," *The Journal of Chemical Thermodynamics*, vol. 125, pp. 41–49, 2018.

[18] E. Beltran, J. L. Serrano, T. Sierra, R. GimΘnez, and R. Giménez, "Tris(triazolyl)triazine via click-chemistry: a C3 electron-deficient core with liquid crystalline and luminescent properties," *Organic Letters*, vol. 12, no. 7, pp. 1404–1407, 2010.

[19] M. Ghasemian, A. Kakanejadifard, F. Azarbani, A. Zabardasti, and S. Kakanejadifard, "The triazine-based azo–azomethine dyes; spectroscopy, solvatochromism and biological properties of 2,2′-((2,2′-(6-methoxy-1,3,5-triazine-2,4-diyl) bis(oxy)bis(2,1-phenylene))bis(azan-1-yl-1-ylidene)bis(methan-1-yl-1-ylidene))bis(4-phenyldiazenyl)phenol," *Journal of Molecular Liquids*, vol. 195, pp. 35–39, 2014.

[20] F. Riobe, P. Grosshans, H. Sidorenkova, M. Geoffroy, and N. Avarvari, "Mono- and bis(tetrathiafulvalene)-1,3,5-triazines as covalently linked donor-acceptor systems: structural, spectroscopic, and theoretical investigations," *Chemistry – A European Journal*, vol. 15, no. 2, pp. 380–387, 2009.

[21] K. Do, H. Choi, K. Lim et al., "Star-shaped hole transporting materials with a triazine unit for efficient perovskite solar cells," *Chemical Communications*, vol. 50, no. 80, pp. 10971–10974, 2014.

[22] Z. F. An, R. F. Chen, J. Yin et al., "Conjugated asymmetric donor-substituted 1,3,5-triazines: new host materials for blue phosphorescent organic light-emitting diodes," *Chemistry - A European Journal*, vol. 17, no. 39, pp. 10871–10878, 2011.

[23] A. Thomas, "Functional Materials: From Hard to Soft Porous-Frameworks," *Angewandte Chemie International Edition*, vol. 49, pp. 8328–8344, 2010.

[24] Z. Wang, C. Liu, Y. Huang, Y. Hu, and B. Zhang, "Covalent triazine framework-supported palladium as a ligand-free catalyst for the selective double carbonylation of aryl iodides under ambient pressure of CO," *Chemical Communications*, vol. 52, pp. 2960–2963, 2016.

[25] A. Bhunia, S. Dey, M. Bous, C. Zhang, W. Von Rybinski, and C. Janiak, "High adsorptive properties of covalent triazine-based frameworks (CTFs) for surfactants from aqueous solution," *Chemical Communications*, vol. 51, no. 3, pp. 484–486, 2015.

[26] L.-C. Lin, J. Choi, and J. C. Grossman, "Two-dimensional covalent triazine framework as an ultrathin-film nanoporous membrane for desalination," *Chemical Communications*, vol. 51, no. 80, pp. 14921–14924, 2015.

[27] Y. Su, Y. Liu, P. Liu et al., "Compact Coupled Graphene and Porous Polyaryltriazine-Derived Frameworks as High Performance Cathodes for Lithium-Ion Batteries," *Angewandte Chemie International Edition*, vol. 54, pp. 1812–1816, 2015.

[28] P. de Hoog, P. Gamez, W. L. Driessen, and J. Reedijk, "New Polydentate and Polynucleating N-Donor Ligands from Amines and 2,4,6-Trichloro-1,3,5-triazine," *Tetrahedron Letters*, vol. 43, no. 38, pp. 6783–6786, 2002.

[29] F. A. I. Al-Khodir, H. M. A. Abumelha, T. Al-Warhi, and S. A. Al-Issa, "Synthesis, chemical and biological investigations of new Ru(III) and Se(IV) complexes containing 1,3,5-triazine chelating derivatives," *Journal of Molecular Structure*, vol. 1179, pp. 795–808, 2019.

[30] R. Xue, H. Guo, T. Wang et al., "Synthesis and characterization of a new covalent organic framework linked by NH linkage," *Materials Letters*, vol. 209, pp. 171–174, 2017.

[31] K. N. Sarmah, N. K. Sarmah, K. B. Kurmi, and T. V. Patel, "Synthesis and studies of antifungal activity of 2,4,6-trisubstituted 1,3,5-triazines," *Advances in Applied Science Research*, vol. 3, no. 3, pp. 1459–1462, 2012.

[32] A. W. Bauer, W. A. Kirby, C. Sherris, and M. Turck, "Antibiotic susceptibility testing by a standardized single disk method," *American Journal of Clinical Pathology*, vol. 45, pp. 493–496, 1996.

[33] M. A. Pfaller, L. Burmeister, M. S. Bartlett, and M. G. Rinaldi, "Multicenter evaluation of four methods of yeast inoculum preparation," *Journal of Clinical Microbiology*, vol. 26, no. 8, pp. 1437–1441, 1988.

[34] G. Repetto, A. del Peso, and J. L. Zurita, "Neutral red uptake assay for the estimation of cell viability/cytotoxicity," *Nature Protocols*, vol. 3, no. 7, pp. 1125–1131, 2008.

[35] W. J. Geary, "The use of conductivity measurements in organic solvents for the characterisation of coordination compounds," *Coordination Chemistry Reviews*, vol. 7, no. 1, pp. 81–122, 1971.

[36] V. Chandrasekhar and S. Nagendran, "Phosphazenes as scaffolds for the construction of multi-site coordination ligands," *Chemical Society Reviews*, vol. 30, no. 3, pp. 193–203, 2001.

[37] A. Solankee, I. Thakor, and J. Indian, "Synthesis ofpyrazolines, isoxazolines andaminopyrimidines as biological potent agents," *Indian Journal of Chemistry*, vol. 45B, pp. 517–522, 2006.

[38] A. A. Khandar and Z. Rezvani, "Preparation and thermal properties of the bis [5- ((4-heptyloxyphenyl)azo)-N- (4-alkoxyphenyl)- salicylaldiminato]copper (II) complex homologues," *Polyhedron*, vol. 18, no. 1-2, pp. 129–133, 1998.

[39] A. Chandrasekaran and S. S. Krishnamurth, "Group VI metal carbonyl complexes of (amino)spirocyclic cyclotriphosphazenes," *Indian Journal of Chemistry*, vol. 33, pp. 391–394, 1994.

[40] R. Ferraro, *Low Frequency vibrations of Inorganic and Coordination Compounds*, vol. 168, Plenum Press, New York, NY, USA, 1st edition, 1971.

[41] R. S. Drago, *Physical Methods in Chemistry*, W.B. Saunders, Philadelphia, Pa, USA, 1977.

[42] A. K. Mishra, S. B. Mishra, N. Manav, D. Saluja, R. Chandra, and N. K. Kaushik, "Synthesis, characterization, antibacterial and cytotoxic study of platinum (IV) complexes," *Bioorganic & Medicinal Chemistry*, vol. 14, no. 18, pp. 6333–6340, 2006.

[43] H. P. Klug, Ed., *X-ray Diffraction Procedures for Polycrystalline and Amorphous Materials*, Wiley, New York, NY, USA, 1974.

[44] S. Krehula and S. Musić, "Hydrothermal Synthesis of Platinum Group Metal Nanoparticles," *Croatica Chemica Acta*, vol. 84, no. 4, Article ID 064620, pp. 465–468, 2011.

[45] S. Navaladian, B. Viswanathan, T. K. Varadarajan, and R. P. Viswanath, "A Rapid Synthesis of Oriented Palladium Nanoparticles by UV Irradiation," *Nanoscale Research Letters*, vol. 4, pp. 181–186, 2009.

[46] Y. Anjaneyalu and R. P. Rao, "Preparation, Characterization and Antimicrobial Activity Studies on Some Ternary Complexes of Cu(II) with Acetylacetone and Various Salicylic Acids," *Synthesis and Reactivity in Inorganic and Metal-Organic Chemistry*, vol. 26, pp. 257–272, 1986.

[47] C. D. Sheela, C. Anitha, P. Tharmaraj, and D. Kodimunthri, "Synthesis, spectral characterization, and antimicrobial studies of metal complexes of the Schiff base derived from [4-amino-N-guanylbenzene sulfonamide] and salicylaldehyde," *Journal of Coordination Chemistry*, vol. 63, no. 5, pp. 884–893, 2010.